Available online at www.sciencedirect.com
ScienceDirect
Journal of the European Ceramic Society 31 (2011) 1611–1617
www.elsevier.com/locate/jeurceramsoc

Injection molding of surface modified powders with high solid loadings: A case for fabrication of translucent alumina ceramics

Wei Liu [a], Zhipeng Xie [a,*], Tiezhu Bo [b], Xianfeng Yang [c]

[a] State Key Laboratory of New Ceramics and Fine Processing, Department of Materials Science and Engineering, Tsinghua University, Beijing 100084, PR China
[b] School of Materials Science and Engineering, University of Science and Technology Beijing, Beijing 100084, PR China
[c] College of Physics and Electronic Science, Changsha University of Science & Technology, Changsha 410114, PR China

Received 30 September 2010; received in revised form 20 February 2011; accepted 1 March 2011
Available online 14 April 2011

Abstract

Solid loading is a critical key to the fabrication of ceramic compacts with high densities via ceramic injection molding. As reported in most previous work, solid loading of ultra-fine alumina feedstock system could be achieved only up to ~58 vol% with stearic acid (SA) as the surface modification agent. In present work, different from the traditional work in which SA has been introduced just in the powder blending process, we have successfully prepared the feedstock with a much higher solid loading up to ~64 vol% by a prior ball milling treatment of ceramic powders with a small amount of SA before the traditional blending process. It can be attributed to that SA can be coated homogeneously around the powder surfaces by a chemical reaction induced by ball milling treatment. Highly translucent Al_2O_3 ceramics have been fabricated, which suggests an alternative route for fabrication of translucent ceramics with high quality.
© 2011 Elsevier Ltd. All rights reserved.

Keywords: Injection molding; Al_2O_3; Optical properties

1. Introduction

Ceramic injection molding (CIM) has stimulated many applications in industry as it can meet the challenge of mass production of small sized and highly complex parts with a near-net formation.[1] One of the key issues for the injection molded compacts is to obtain a high solid loading in the feedstock system. There are different methods to increase solid loading, i.e., Liang et al. added proper ratio of CNTs to increase the powder loading of MIM feedstock about 10%.[2] Thomas et al. established the optimum powder loading by means of torque and rheological measurements of different feedstock formulations.[3] Liu pointed out that a careful selection of ceramic powder/binder systems could be quite helpful to obtain high solid loading.[4] Besides, the use of a high-performance dispersing instrument would also increase solid loading.

In addition, one of the most effective ways is to utilize surface modification agent to make a chemical reaction and achieve excellent homogeneity among the neighbored particles to overcome the poor compatibility between the ceramic powders and organic binders.[5–8] Tseng et al. reported that the alumina feedstock rheology and the green microstructure of injection-molded ceramic-binder mixtures may be engineered by means of surface active additives.[6] Wang et al. adopted SA as surface modification agent to improve the binder chemistry, which changed the ceramic powders from hydrophilicity to hydrophobicity.[7] Such routes could lead to effective reduction of the suspension viscosity, good wetting and strong adhesion between the binders and powders.[9–10] Consequently, high solid loading of the feedstock system could be achieved,[6,9] which could result in fabrication of injection-molded compacts with high densities.[11,12]

However, as reported in most previous work, solid loading of ultra-fine alumina feedstock system could be achieved only up to ~58 vol% with SA as surface-active agent,[3] in which SA was introduced just in the powder blending process. In current work, we report an improved route for introduction of surface-active agent by a prior ball milling treatment of ceramic powders with a small amount of SA before the blending process. We find that the prior ball milling treatment can result in good chemical coating of SA on the surface of ceramic powders, obtaining the

* Corresponding author. Tel.: +86 10 6279 9031; fax: +86 10 6277 1160.
E-mail address: xzp@mail.tsinghua.edu.cn (Z. Xie).

0955-2219/$ – see front matter © 2011 Elsevier Ltd. All rights reserved.
doi:10.1016/j.jeurceramsoc.2011.03.003

Table 1
Characteristics of pure alumina.

Content of α-phase (%)	BET (m^2/g)	Average particle size (μm)	Max. particle size (μm)	Purity (%)
99	6–10	≤0.5	≤4	≥99.98

Table 2
Compositions of organic binders.

	Components				
	PP	EVA	PW	SA	DBP
Volume (%)	10	10	60	15	5

feedstock with a much higher solid loading up to ~64 vol%. Subsequently, translucent alumina ceramics with high quality have been fabricated by using the surface modified powders.

2. Experimental procedure

2.1. Materials

Commercially available α-alumina powders (Zichuan Phoenix Precision Ceramics Co., Ltd., China) have been used for the raw materials. The detailed characteristics of the powder used are shown in Table 1. A muti-component binder system was selected for our work. The used organic vehicles (binders) in the experiments were: polypropylene (PP, K8303, Beijing Yanshan Petrochemical Co., Ltd., China), Ethylene-Vinyl Acetate Copolymer (EVA, VA content was 14%, Beijing Chemical Factory, China), paraffin wax (Shenyang Paraffin-wax Chemical Co., Ltd., China), stearic acid (SA, Shantou Xilong Chemical Factory Guangdong, China) and dibutyl phthalate (DBP, Beijing Modern Eastern Fine Chemical) with the compositions shown in Table 2. TGA analysis of binder components is shown in Fig. 1.

2.2. Powder pretreatment

As the most key step in our work, the powders should first be surface modified by SA with various contents from 1 wt% to 4 wt% via wet ball milling in a planetary ball mill for 6 h (QM-3SP2, Instrument Factory of Nanjing University, China). And at the same time, the additives of MgO and Y_2O_3 with small amount were introduced into the powders in the form of nitrate to retard abnormal crystal growth in the sintering process followed. As it is for ball milling, the powders were mixed with alcohol and alumina balls. Two kinds of ceramic milling balls (diameter of 5 mm and 6 mm, respectively) were used with weight ratio of 1:1. The ball-milling system consists of powders/alcohol/ball in the weight ratio 1/1/2. The resultant powders were dried at 40 °C in air condition. For comparison, the pure Al_2O_3 powder and the modified one were referred to Powders 1# and 2# respectively in the following discussion.

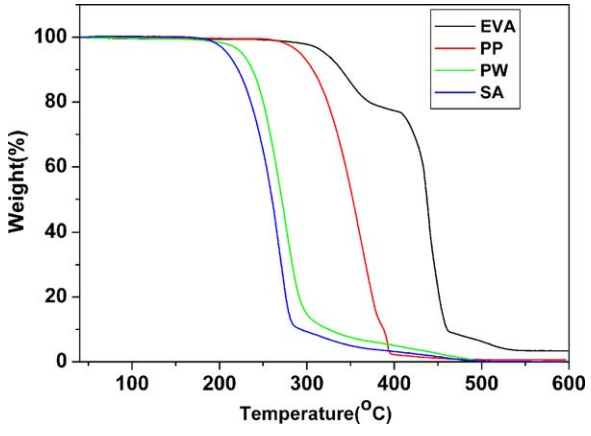

Fig. 1. TGA analysis of binder components.

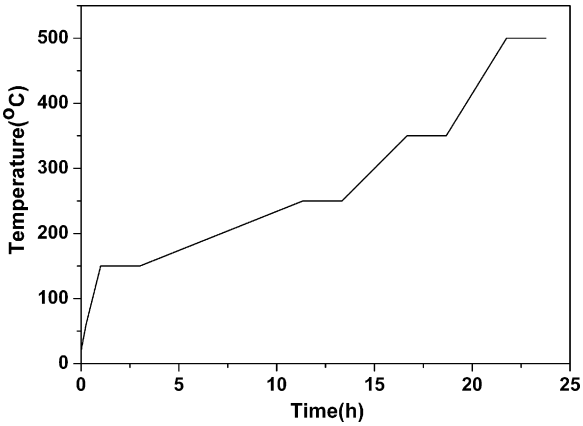

Fig. 2. The heating schedule adopted for the debinding process.

2.3. Mixing

A twin screw kneader (SK-160, ShangHai Rubber Machinery, China) was used with a mixing bowl of 2 L and operated at a rate of 11 rpm. In the beginning of the kneading process, PP and EVA was heated to 170 °C in the kneader. The other ingredients were then added in a sequence as indicated below: alumina was first added to form a mixture. After mixing for 15 min, PW and SA were gradually added in the kneader. Finally, DBP as a plasticizer was slowly added into the mixture. The whole mixing process lasts about 40–50 min.

2.4. Injection molding

The specimens were fabricated on an injection molding machine (JPH30C/E, Qinchuan Hengyi Plastics Machinery Co. Ltd., China). The barrel temperatures of the IM machine from feeding to sprue side were 155–160–165–170 °C. The injection pressure and time were 50 MPa and 3 s, respectively. The holding pressure and time were 50 MPa and 6 s, respectively. In addition, the cooling time and the mold temperature were set at 6 s and 50 °C respectively. The dimension of the molded specimens was Φ22 mm × 1.2 mm.

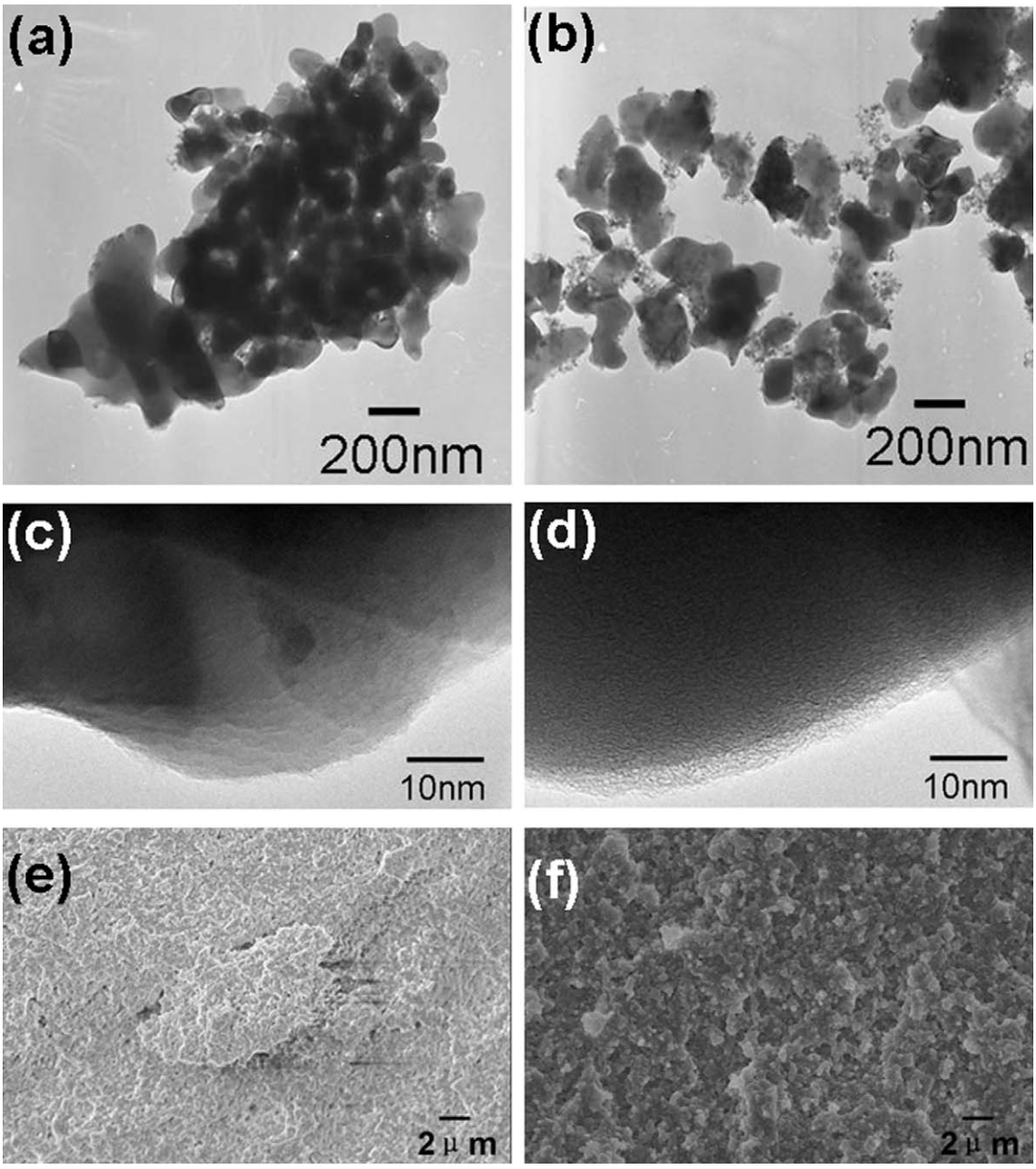

Fig. 3. (a and b) Typical TEM images of Powder 1# and Powder 2#, respectively. (c and d) Typical HRTEM images of Powder 1# and Powder 2#, respectively. (e and f) Microstructures of the compact (58 vol%) made from Powder 1# and Powder 2#, respectively.

2.5. Debinding and sintering

The as-prepared compacts were debound in a muffle furnace with the heating schedule indicated in Fig. 2. The debinding process is carried out in air atmosphere with a slow heating rate, thus most of carbon in green body could be removed.

The grown bodies were then sintered at 1830 °C for 3 h in a H_2-atmospher furnace (LHT04/17, Nabertherm, Germany) with a heating rate of 150 °C/h.

2.6. Characterization

Thermo-gravimetric analysis (TGA) was conducted on the DSC/TG analyzer (STA 409 PC/PG, Netzsch, Germany) at a heating rate of 10 °C/min up to 600 °C in air atmosphere. The rheological behavior of the mixtures was characterized with a capillary rheometry (canton, Instron model 3211, England). The chemical characteristics of alumina powders with and without surface modification were analyzed by Fourier transformation infrared spectrometer (FTIR-6700, Nicolet, USA) operated from

4000 to 400 cm^{-1}. The transmission spectrum of the polished sample with the thickness of 0.8 mm was measured in the wavelength 300–800 nm using a UV–VIS spectrophotometer (U-3310, Hitachi). The morphology of the green body and sintered body was observed by Field emission scanning electron microscopy (FESEM, LEO1530, German) operated at 5 kV. SEM samples of the sintered bodies were thermally etched at 150 °C lower than the sintering temperature for 30 min followed by being polished using diamond paste. All the SEM samples were diposed on a graphite paper and then covered by a thin layer of gold. The dispersity of the powders was characterized by transmission electron microscopy (TEM, H-800, Hitachi, Japan) operated at 200 kV. The surface of the powder was characterized by high resolution transmission electron microscopy (HRTEM, JEM-2010, JEOL, Japan) operated at 120 kV. TEM samples (powders) were finely dispersed in ethanol using ultrasonic treatment and then dropped onto holey-carbon-coated copper grids. The bulk densities of the sintered specimens were measured by the Archimedes method.

3. Results and discussion

Fig. 3(a and b) shows the respective TEM images of Powder 1# and Powder 2#, indicating Powder 2# was better dispersed without agglomeration as compared with Powder 1#. Fig. 3(c and d) responds to HRTEM images of Powder 1# and Powder 2#, respectively, disclosing the microstructure evaluation of the powders after surface modification. It suggests that the particle surface was surrounded by an amorphous monolayer. Though it is difficult for us to completely confirm the amorphous layer being of SA due to the very low melting point and extremely thin layer of SA (~3 nm), we have proved that there is a chemical reaction (esterification) occured between the particle and SA, in which Al–O–CO band has formed induced by the treatment of ball milling based on the following FTIR analysis.[5,13–15] Hence the characteristic of treated SA is quite different from pure SA including the melting temperature, for there is a strong interaction between SA and the powder. Thus, the coating seems to be SA. Fig. 3(e) and (f) are the typical SEM images of the compacts using Powders 1# and 2#, respectively. They display that the microstructure of the compact by using Powder 2# is much more homogeneous than that by Powder 1#, implying that the agglomeration of the particles can be limited by the surface modification of SA. The agglomeration of the Powder 1# particles can be attributed to the nature of the ceramic powder surface, which is generally polar and hydrophilic and leads to the poor affinity between the ceramic powders and organic binders. Consequently, the bonding strength between ceramic particles and organic binders decreases, causing ceramic particles and organic binders to separate easily during the process of high-speed and high-pressure injection molding.[16] However, the particles of Powder 2# have been surface modified by SA, which enhances the bonding strength between the ceramic particles and organic binders, and results in the fabrication of the compacts without agglomeration.

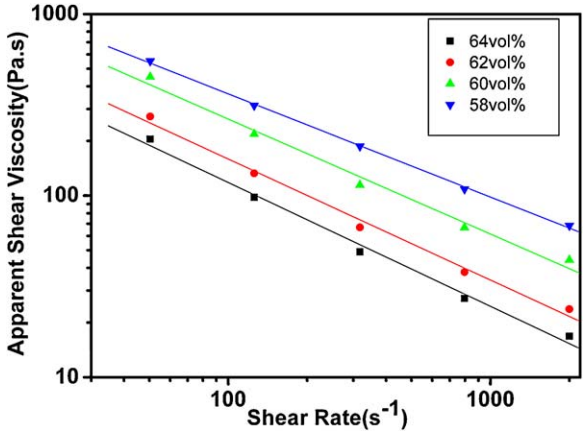

Fig. 4. The apparent shear viscosity versus the shear rate for different solid loadings (58–64 vol) of Powder 2# at 170 °C.

Fig. 4 responds to the apparent shear viscosity versus the shear rate for different solid loadings (58–64 vol) of Powder 2# at 170 °C (The temperature adopted for injection molding), showing a pseudoplastic behavior. Excellent rheological properties were obtained because it has been stated that a viscosity of less than 1000 Pa s within the shear rate range 100–1000 s^{-1} can be regarded as a usable formulation by Edirisinghe et al.[17]

Fig. 5(a) is the infrared absorption spectrum of Powder 1#. 3420 cm^{-1} is defined to be the vibration peak of hyroxy, which shows that the surface of alumina powder is rich in hydroxyl groups and provides the possibility of esterification with SA. Fig. 5(f) is the infrared absorption spectra of SA, in which bands centered at 2920 and 2850 cm^{-1} are the antisymmetrical and symmetrical stretch vibration absorption spectra of CH_2, respectively. There is a strong absorption peak at 1750 cm^{-1}, owning to carbonyl stretching vibration of SA; Fig. 5 (b–e) is the infrared absorption spectrum of Powder 2# with different additions of SA. Compared with Powder 1#, there are new absorption peaks at 2920 cm^{-1}, 2850 cm^{-1} for Powder 2#. In

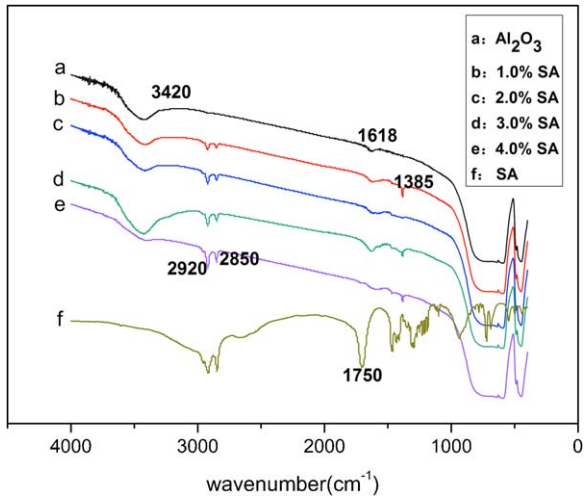

Fig. 5. (a–f) Infrared absorption spectra of Powder 1#, Powder 2# with 1.0 wt% SA, Powder 2# with 2.0 wt% SA, Powder 2# with 3.0 wt% SA, Powder 2# with 4.0 wt% SA, and pure SA, respectively.

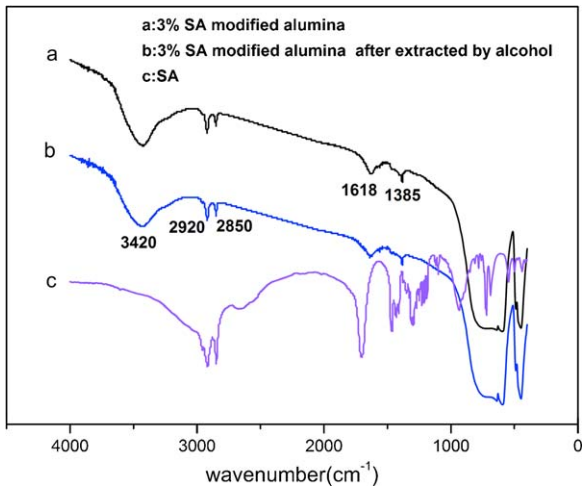

Fig. 6. (a–c) Infrared absorption spectra of Powder 2# with 3 wt% SA, Powder 2# with 3 wt% SA extracted by alcohol, and pure SA, respectively.

addition, 1704 cm^{-1} in Fig. 2(d) corresponds to stearic acid carbonyl stretching vibration, while the same peak of the carbonyl stretching vibration in Fig. 2(b) and (c) shifts to the 1618 cm^{-1}. It illustrates that the carbonyl linked group changed through modification. The intensity of the absorption peak gradually increases with the increment of SA concentration, implying different contents of SA have been coated on the surface of the powders. To confirm whether it is a physical coating or a chemical coating, Powder 2# was washed by hot ethanol which can dissolve SA with ultrasonic vibration, air pump filtration and then dried. The infrared absorption spectra of the powders corresponding to respective Powder 2# with 3 wt% SA, Powder 2# with 3 wt% SA extracted by alcohol, and pure SA, are shown as Fig. 6. 1618 cm^{-1} and 1385 cm^{-1} are for the carbonyl(C=O) stretching vibration peak and the stretching vibration peak of C–O–C, respectively. It demonstrates that Al–O–CO band forms through such modification.[5,13–15] The above FTIR analysis evidences that SA has been coated on the surface of the powder through a chemical reaction (esterification) instead of physical adsorption.

Highly translucent Al_2O_3 ceramics have been successfully fabricated by injection molding of the surface modified powders followed by sintering in H_2 atmosphere at 1830 °C. The real in-line transmission% (RIT %) of each sample produced by Powder 1# and Powder 2# of different solid loadings is shown in Fig. 7(a). It seems that poor translucency is obtained by using Powder 1#, for its real in-line transmission is not satisfactory. By contrast, the samples prepared from Powder 2# possess higher translucency. The real in-line transmittance of the prepared translucent Al_2O_3 ceramics (64 vol%) can be up to 15.3% within the UV–VIS light region. The transparency slightly increases with the increment of solid loadings from 58 vol% to 64 vol%. It suggests that solid loading is critically important for the fabrication of the translucent Al_2O_3 ceramics by CIM, for the density of sintered body will be higher with the increment of the solid loading in green compact.[18] Surface modification of the powders induced by prior balling milling treatment can limit the agglomerate formation of ultrafine powders, lead to a chemical reaction and obtain excellent homogeneity among the neighbored particles to overcome the poor compatibility between the ceramic powders and organic binders,[5–8] which result in a higher solid loading attainable for a given powder. Meanwhile, since SA adsorbed chemically onto the powder surface changes the flow behavior of the mixtures from a dilatant flow to a pseudoplastic one at low temperatures with a yield stress,[5] it increases exponentially with decreasing particle-particle separation and makes the particles arrange in an ordered dense packing configuration.[19] For Powder 1#, the maximum solid loading is only 58 vol%, while that of Powder 2# can be up to 64 vol%. It implies that our method for powder surface modification can improve the maximum solid concentration, and subsequently increase the relative density (T.D.%) of the sintered sample as shown in Fig. 7(b), which results in the fabrication of Al_2O_3 ceramics with higher translucency. It is worth noting that the relative density of Powder 2# is obviously higher than that of Powder 1#, which is consistent with the above analysis on the effect of SA surface modification. In addition, there is an increasing trend in the relative density with the enhancement of the solid loading for Powder 2#, since a homogeneous and dense particle packing enhances the sintering behavior and leads to a higher sintered density.[20] Fig. 7(c) depicts the fabricated dental parts by using Powder 1#(i) and 2#(ii) (58 vol%). The samples have not been treated by any subsequent processing such as grinding and polishing, suggesting

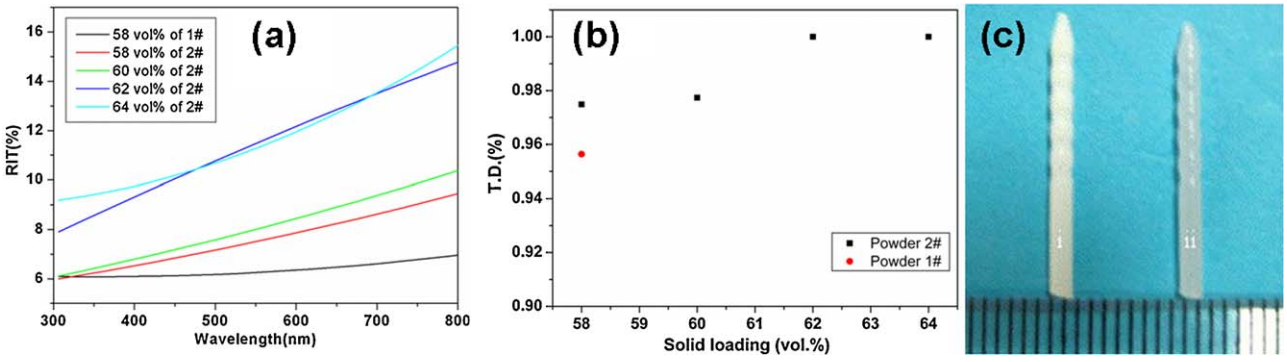

Fig. 7. (a) The real in-line transmittance (%) versus wave length (nm) in the visible light region of all the sintered samples with the thickness of 0.8 mm (b) The relative density (T. D. %) of all the sintered samples (c) Respective dental parts made from Powders 1# and 2#. The solid concentration of the sample is 58 vol%.

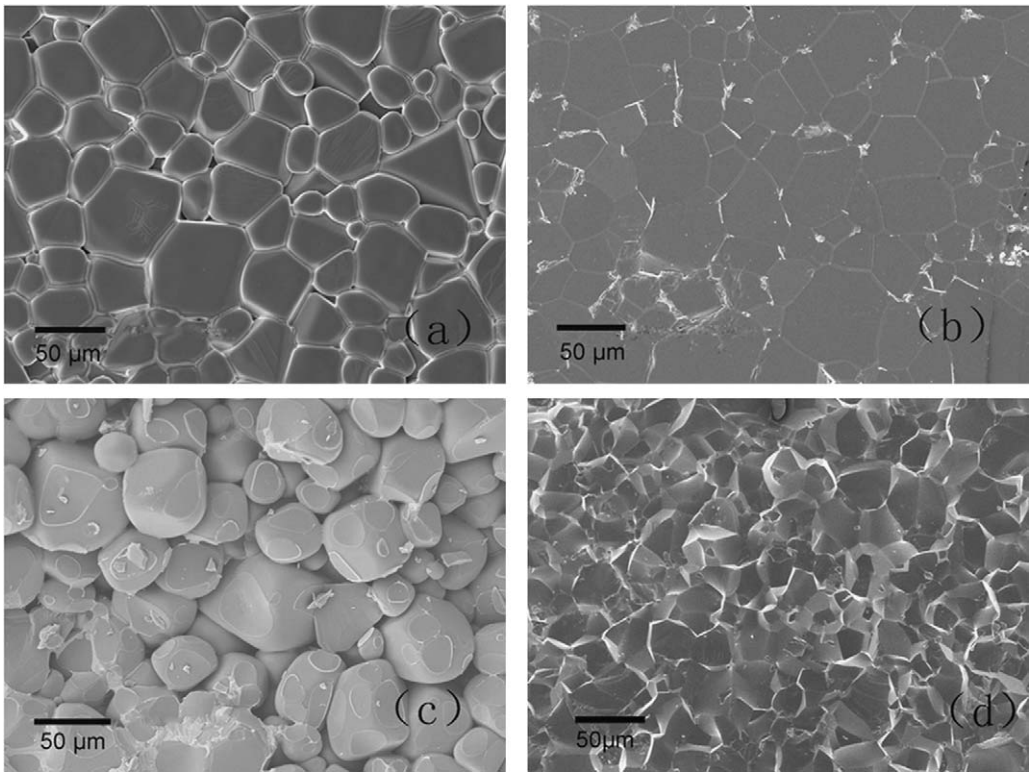

Fig. 8. (a) The microstructure of the polished surface of the sintered sample with a 58 vol% solid loading made from Powder 1#, (b) the microstructure of the polished surface of the sintered sample with a 58 vol% solid loading made from Powder 2#, (c) the corresponding cross section of the fracture surface made from Powder 1# and (d) the corresponding cross section of the fracture surface made from Powder 2#.

that the dental parts with high quality can be fabricated via CIM by using surface modified Al_2O_3 powders.

Fig. 8(a) and (b) are the microstructures of the polished surface of the sintered sample with a 58 vol% solid loading made from Powders 1# and 2#, respectively. Fig. 8(c) and (d) are corresponding cross section of the fracture surface. It shows that the pores of the sample made from Powder 2# are much less than those made from Powder 1#, which results from improved relative density through surface modification, in turn, leading to a higher translucency of the fabricated Al_2O_3 ceramics.

4. Conclusions

We have reported a strategy to greatly improve solid loading for ceramic injection molding by a prior ball milling treatment of ceramic powders with a small amount of SA. SA can be coated homogeneously around the powder surfaces by a chemical reaction induced by the ball milling treatment, which makes excellent homogeneity among the neighbored particles to overcome the poor compatibility between the ceramic powders and organic binders. Highly translucency Al_2O_3 ceramics have been successfully fabricated by injection molding of the surface modified powders followed by sintering in H_2 atmosphere. The real in-line transmittance of the prepared transparent Al_2O_3 ceramics (64 vol%) can be up to 21.3% within the UV–VIS light region, suggesting that current work might provide an alternative route for the fabrication of translucent ceramics with high quality.

Acknowledgements

This work was financially supported by "The High Technology Research and Development Program" of China ("863" Program, Grant No. 2007AA03Z522) and the National Nature Science Foundation of China (NSFC).

References

1. Gulsoy HO, German RM. Production of micro-porous austenitic stainless steel by powder injection molding. *Scripta Mater* 2008;**58**:295–8.
2. Liang SQ, Tang Y, Zhang Y, Zhong J. The rheologyical effect of carbon nanotubes on the iron based metal powder injection molding feedstock. *Multi-Functional Mater Struct II* 2009;**79–82**(Pts 1 and 2): 469–72.
3. Thomas-Vielma P, Cervera A, Levenfeld B, Varez A. Production of alumina parts by powder injection molding with a binder system based on high density polyethylene. *J Eur Ceram Soc* 2008;**28**:763–71.
4. Liu DM. Influence of solid loading and particle size distribution on the porosity development of green alumina ceramic mouldings. *Ceram Int* 1997;**23**:513–20.
5. Chan TY, Lin ST. Effects of stearic-acid on the injection-molding of alumina. *J Am Ceram Soc* 1995;**78**:2746–52.
6. Tseng WJ, Liu DM, Hsu CK. Influence of stearic acid on suspension structure and green microstructure of injection-molded zirconia ceramics. *Ceram Int* 1999;**25**:191–5.
7. Wang L, Yang X, Zhang Z, Xie Z. Mechanism of thermal debinding and water debinding for ceramic injection molding. *Rare Met Mater Eng* 2007;**36**:330–3.
8. Wright JK, Edirisinghe MJ, Zhang JG, Evans JRG. Particle packing in ceramic injection-molding. *J Am Ceram Soc* 1990;**73**:2653–8.

9. Gutierrez JAE, Fredel MC, Wendhausen PP, Klein AN. Preparation of hard metal (WC-10Co) components by powder injection moulding. *Key Eng Mater* 2001;**189**(1):579–85.
10. Lin ST, German RM. Interaction between binder and powder in injection-molding of alumina. *J Mater Sci* 1994;**29**:5207–12.
11. Sacks MD, Khadilkar CS, Scheiffele GW, Shenoy AV, Dow JH, Shen RS. In: Messing GL, Kazdiyasni KS, McCauley JW, Harber RA, editors. *Ceramic powder science*, 11. Westervillea, OH: American Ceramic Society; 1987.
12. Zhang JG, Edirisinghe MJ, Evans JRG. The use of silane coupling agents in ceramic injection moulding. *J Mater Sci* 1988;**23**:2115–20.
13. Wolfrum SM, Ponjee JJ. Surface modification of powders with carboxylic-acids. *J Mater Sci Lett* 1989;**8**:667–9.
14. Wu RY, Wei WCJ. Torque evolution and effects on alumina feedstocks prepared by various kneading sequences. *J Eur Ceram Soc* 2000;**20**:67–75.
15. Liu J-C, Jean J-H, Li C-C. Dispersion of nano-sized γ-alumina powder in non-polar solvents. *J Am Ceram Soc* 2006;**89**:882–7.
16. Aggarwal G, Park SJ, Smid I. Development of niobium powder injection molding. Part I. Feedstock and injection molding. *Int J Refract Met H* 2006;**24**:253–62.
17. Edirisinghe MJ, Evans JRG. Properties of ceramic injection moulding formulations. *J Mater Sci* 1987;**22**:269–77.
18. Liu DM, Tseng WJ. Rheology of injection-molded zirconia-wax mixtures. *J Mater Sci* 2000;**35**:1009–16.
19. Ivensen VA. *Densification of metal powders during sintering*. New York: Consultants Bureau; 1973.
20. Paul Lin ST, German RM. The influence of powder loading and binder additive on the properties of alumina injection-moulding blends. *J Mater Sci* 1994;**29**:5367–73.